# Prefabricated and Assembled Electromagnetic Shields Inside Electronic Packages to Reduce Near-Field Capacitive and Inductive Coupling

Ghaleb Saleh Ghaleb Al-Duhni, *Graduate Student Member, IEEE*, Mudit Khasgiwala, John. L. Volakis, *Life Fellow, IEEE*, and Pulugurtha Markondeya Raj, *Senior Member, IEEE* 

Abstract-Electromagnetic shielding often requires the integration of thick shielding structures in the form of metal casings, walls, or via arrays. These shields typically isolate the entire package from external or internal noise sources. In some cases, they also isolate components within the package. However, integration of shielding structures with the required performance creates miniaturization and fabrication constraints, and results in longer product development cycle times. To address these limitations, a novel approach is presented for component- and package-level shielding. This approach electromagnetic interference (EMI) shield integration through a microassembly of prefabricated shields inside microslots in packages and printed circuit boards (PCBs). This approach eliminates many of the design and process constraints during the shield integration within packages. Various design options were considered to mitigate capacitive and inductive coupling between representative microstrip lines that act as aggressors and victims. Three types of EMI shielding architectures, U-shaped, inverted-Lshaped, and T-shaped, were investigated with 17.5 µm copper. The fabricated EMI shields were studied for their shield performance, both as a compartmental shield between specific components and as a conformal shield from external and internal noises. The role of the ground termination was also investigated to further optimize the shielding performance.

Index Terms—Compartmentalized shield, Conformal shield, Monolithic copper, Prefabricated and assembled EMI shielding, and Thin and thick EMI shielding.

#### I. INTRODUCTION

lectromagnetic compatibility (EMC) is becoming a key upfront design requirement for future electronics. Meeting EMC requirements becomes challenging as component and functional densities increase with performance and miniaturization trends. Electromagnetic Interference (EMI) issues originate from different sources depending on the subsystem functions [1, 2]. Irrespective of the noise source, the reduced spacing between the components in future electronic systems leads to enhanced electromagnetic interactions and will require innovative solutions to address them [3-8]. In the case of power electronic systems, EMI is a

key concern because key circuit elements such as switches, inductors, and return current loops act as noise aggressors. The high-frequency harmonics that originate because of the sharp rise times are a major source of this noise. Noise is often coupled through the mutual impedance in the return current path. Implementing effective electromagnetic interference (EMI) shielding inside electronic packages is critical to address these concerns [9, 10]. Regulatory immunity requirements due to emissions from all unintended radiators create additional EMC constraints. In the category of RF subsystems, EMI is a concern because of the coexistence of several bands such as 2400 MHz Bluetooth, 2450 MHz Wi-Fi, 1575 MHz for GPS, 900 MHz, and 1800 MHz for GSM [6], amongst others. Interference between these RF channels and with the power supply harmonics can lead to degradation and even malfunction in the RF performance [11-13]. In the other category of computing systems, the trend in digital circuits to use higher clock frequencies and fast edge switches also results in more noise [14, 15]. Unintended radiation sources originate from any digital device that has a clock with an operating frequency of more than 9 kHz per federal regulation the Code of Federal (CFR) Regulations, which encompasses all EMC regulations issued by the Federal Communications Commission (FCC) under Title 47 of the CFR [1].

Several types of EMI shields are used in electronic systems at the IC and package levels. Shield encasings at the package level are the most common types and are used in the form of metal cans or metal lids [7, 16]. Metal cans are known for their excellent shielding performance [6, 16, 17]. However, they have limitations in terms of their footprint, thickness, and complexity of the implementation inside electronic packages. They lead to larger packages by 14% and expand the footprint by 15% [7]. In addition, they increase fabrication and assembly costs [6, 18].

Conformal EMI shielding is the most promising technology for reducing the thickness and weight of electronic packages [6, 8, 11, 17, 18]. This was predominantly applied to isolate the noise from the digital and RF circuits in mixed-signal packages [19]. They are deposited by spray-coating metal slurries or inks, physical vapor deposition such as sputtering, or electrochemical solution deposition techniques such as electroless and

electrochemical plating [11]. They often compromise the shielding performance for several reasons. For example, sputtering leads to thickness limitations and stress issues. Being a line-of-sight technique, it also leads to nonuniform coatings on the sidewalls. Deposition through paste, liquid, or slurry coating of composites limits the conductivity of the shield materials [6, 20]. Electroless and electroplating techniques impose process constraints and compatibility issues with the mold compounds. However, all these techniques have been sufficiently advanced through decades of research to meet the shielding requirements and are widely adapted by industry and investigated by academia. Various designs and configurations are utilized for conformal shields to mitigate far-field [6, 8] and near-field coupling [7, 16-19, 21, 22] with advanced materials and processes. Selected highlights are provided in Table I.

One of the main limitations of conformal EMI shielding is the ability to shield components within the same package. This is referred to as compartmental EMI shielding [6] and is usually created with metal partitions as walls or via arrays at the package or PCB level [23, 24]. Several other reports investigated this technology and are briefly highlighted next. Three design variants of EMI shielding, viz., L, U, and zigzag shapes, are used in LTE SiP modules. The compartment shields showed better performance as compared to the traditional metal lid by shielding with 50 dB isolation up to 6 GHz [25]. In [5], a spray-coating technology was used for SiP modules with a shielding effectiveness of 30 - 55 dB across 0.5-6 GHz. For this case, the coating thickness varied from 3-11.6 µm. To address near-field coupling, mold-based compartment shielding was employed to reduce intra-package noise within components by 30 dB [6]. A trench-filled compartment shield using a conductive paste showed shielding effectiveness of 40 dB with a thickness of 140 µm across 1.6-2.6 GHz [9].

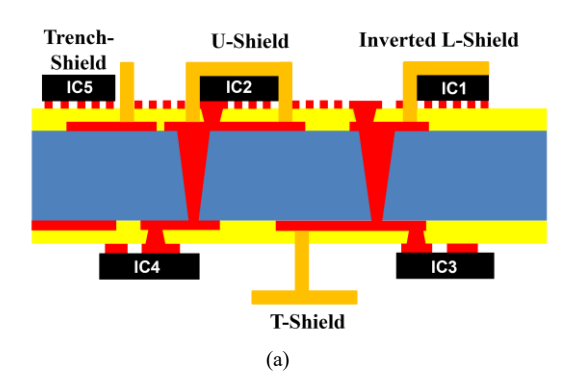
As stated in [7, 17-19, 21, 22], conformal EMI shields are predominant in today's electronic packages. But they must be eventually extended to compartmentalized shields as mentioned in [5, 6, 9, 25] to protect future packages from external and internal noise. However, the combination of shielding techniques adds fabrication cost, thickness, height, and process development time. Notably, achieving higher shielding effectiveness from far-field coupling is less challenging as compared to near-field coupling [5, 6, 8, 25], the latter posing a key concern. All these requirements add challenges to the shielding process.

To address the aforementioned limitations, we present a novel approach for component- and package-level shielding using a simpler fabrication. This approach is based on the microassembly of prefabricated EMI shields inside microslots in printed circuit boards (PCBs). Such an approach leads to fewer design and process constraints during fabrication because the process does not need to follow additional steps for deposition and patterning. Therefore, it is more adaptable to various shield geometries and materials and lowers the fabrication cost by simplifying the integration process. This approach can lead to many design, fabrication, and performance advantages: 1) Shielding architectures can simultaneously address both conformal and compartmentalized shielding. They can have several shapes instead of being a plated or trench-filled wall or via. 2) Optimal shapes can be designed with flexible

layouts compared to the usual metal enclosures. 3) Shield dimensions and thickness can be designed independently of substrate wiring design rules. 4) Assembled or inserted shields are more effective in terms of cost at the product level as they shorten design and product development cycles. 5) Compartmentalized and conformal shielding can be designed independently, thus providing ease in fabrication and assembly. The prefabrication and assembly approach allows optimized material stacks for each application.

I ABLE I
INTEGRATED SURVEY OF CONFORMAL AND COMPARTMENT EMI
SHIELDING TECHNIQUES ACROSS FREQUENCIES: SYNTHESIZING
MULTIPLE REFERENCES.

Reference	Frequency (MHz)	Shielding (dB)	Material/Method			
Conformal EMI shielding						
5	30-3000	90	Nanosilver filler coating (8-20 µm)			
6	1000-6000	36-50	40 nm anti-oxide layer and 1 μm Copper			
7	=	7 more than traditional metal EMI shield	Side-wall opening to avoid internal resonance of the shield			
16	10-5800	11-44	Innovative adhesion enhancement based on a simultaneous mechanical anchoring process and chemical interaction (20 µm)			
17	-	40	Silver material sprayed onto a plastic mold of SiP			
18	-	20	Electroless-plated Copper (5 µm)/Ni (7 µm) stack-up			
19	10	19-28	Cu/NiFe stack (10-18 µm)			
21	5000	43	Metal ink-derived shield (4-5 μm)			
22	1	6-26	Magnetic sheet and conductive silver (98- 500 μm)			
	Comp	artment EMI Shield	ling			
5	500-6000	30-55	Spray-coating technology for SiP modules (3-11.6 μm)			
6	-	30	Mold-based compartment shielding			
9	1600-2600	40	Trench-filled compartment shield using conductive paste (140 µm)			
26	5800	35	Electroplated soft magnetic metal and high-conductive copper			
27	0-6000	20-40	Tooth-shaped compartment shielding technology			
28	20,000- 40,000	20-40	Compartment shielding, which utilized conductive adhesive filling technology inside cavities			



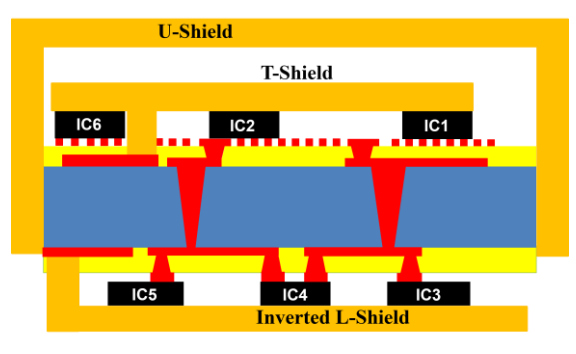
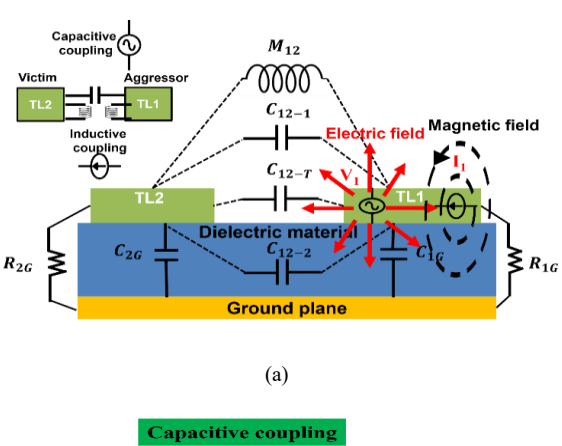


Fig. 1. EMI shielding shapes depicted in 2D schematics: a) Compartmental, and b) Conformal EMI shielding: Trench, Inverted L-shaped, T-shaped, and U-shaped.



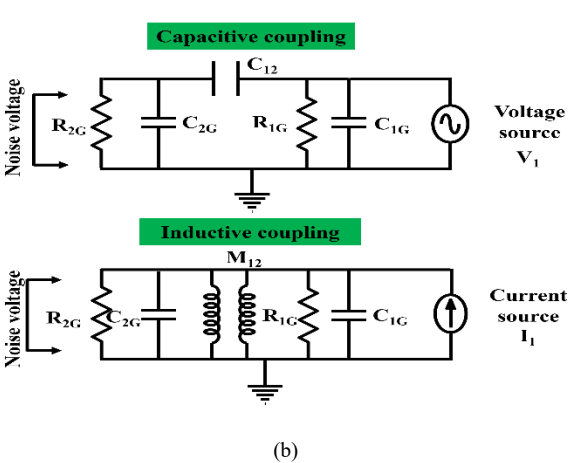


Fig. 2: Equivalent circuit of the near field coupling in the proposed prototypes: a) physical representations, and b) schematic representations.

This work aims to study the performance of various conformal and compartment shield designs such as U, Inverted L, T, and other shapes. Only Copper (Cu)-based shields are considered in this work although the fabrication method could be applied to other emerging shielding materials. Near-field capacitive and inductive coupling between components is emulated as cross-talk between transmission lines (TLs) to demonstrate isolation. Finally, the impact of the grounding termination of the shield on the EMI shielding performance is also studied. The shield and test structures are illustrated in Fig. 1.

### II. EMI SHIELDING DESIGNS

Noise sources and victims are represented as microstrip line test structures in order to study the performance of conformal and compartment shields through modeling and hardware validation. To study the capacitive and inductive coupling between the TLs, it is simpler to understand them as lumped components with mutual capacitance and inductance. The pickup noise voltage increases as the voltage and frequency at the source increase. Furthermore, the noise voltage is directly proportional to the mutual capacitance between the TLs and the resistance from TL2 to the ground. The mutual capacitance  $(C_{12})$  between the lines increases as the width and the length of the coupling conductors increase. Also, it decreases as the ratio between the spacing and width of the conductive traces increases. The noise voltage sensed by the shield depends on the mutual capacitance between the shield and the source  $(C_{1s})$ . However, that has no significant impact on the pickup noise voltage at TL2 even though  $(C_{12})$  is reduced in the presence of the shield. Noticeable impact in reducing the noise voltage is only seen when the shield is terminated to the ground, where the leakage capacitive coupling between the shield and the victim is reduced. This ideally leads to the elimination of the pickup noise voltage at TL2. Nevertheless, termination between the ground and shield can add parasitic impedances from inductances and apertures in the shields.

Shielding of magnetic fields is determined by the inductive coupling from the mutual inductance ( $M_{12}$ ) between the two TLs. The pickup voltage on the victim IC depends on the flow current in the aggressor TL denoted by  $I_1$ . The effectiveness of the shield in suppressing inductive coupling originating from the induced magnetic fields in the shield. These fields will cause a current in the shield to flow in the direction opposite to that in the aggressor line. Therefore, the induced current generates a magnetic field that opposes the corresponding field from the aggressor. When the metallic shield is shunted to the ground, it is expected to suppress the capacitive and inductive coupling noise to zero. To achieve this, the shield has to cover the aggressor line completely and be terminated to the ground. Similar to the capacitive coupling of electric fields, the noise voltage will not be eliminated because of the complex field coupling through apertures and imperfect shields. Therefore, a 3D model using Ansys® HFSS was used to study the impact of the assembled and prefabricated EMI shielding on mitigating near-field noise from capacitive and inductive coupling (see Section VIII). The equivalent circuit for the near-field coupling

between the TLs is illustrated in Fig. 2.

Several shielding designs are considered. Trench-based shields are the simplest option and are viewed as 1-faced shields. This shielding approach incorporates a metal wall between electronic components that are terminated to a ground plane. The second variation employs a T-shape, effectively a two-faced EMI shield. These T-shaped shields cover the victim and source in two directions (X and Y). The third approach is referred to as an Inverted L-shaped EMI shield. It has 2 faces but focuses either on the victim or the source. The fourth EMI shield is a U-shape enclosure that has 3 faces. These four approaches could be extended as 4, and 6-face (Box) EMI shielding approaches. As shown in Fig. 1, compartment and conformal EMI shielding can take any of the previously mentioned shapes.

## III. EMI SHIELDING TEST STRUCTURES AND FABRICATION

The process of prefabricated and assembled EMI shielding for conformal and compartment shields is depicted in Fig. 3. The first and second steps are standard for any copper-clad substrate. The key processes for these two steps to form the circuit patterns are photolithographic patterning and subtractive etching. The third step is that of building up dielectric layers through polymer film lamination onto the top of the conductive layer. This is followed by creating slots or trenches, using CO<sub>2</sub> laser machine. The shield is prefabricated through a separate process with diced copper traces and assembled to the required shapes. As stated previously, a simple structure of two-metallayered PCB was used in this work. The structure has three microstrip lines, with a length of 30 mm and a width equal to 3mm. The separation distance between the lines is 6 mm. The line in the middle is used as the aggressor (source of the noise) and one of the lines in the sides is used as the victim (receptor of the noise). The dimensions of the shields range from 7.5 - 30 mm in the lateral and transverse direction, and 200 µm in the orthogonal direction that is inserted into the slot. These shields are, thus, integrated with the coupled TL structures. Design variations such as T, Inverted L, and U-shape are studied. Assembly and grounding of the shield are the key steps. Therefore, a solder paste is used to interconnect the shield to the ground plane of the package substrate via a reflow soldering process. In addition, an adhesive layer is also needed to assemble the shield inside the slot with good mechanical integrity, as shown in Fig. 3. Thus Step 5 is implemented by depositing an adhesive layer onto the package trenches or the prefabricated shields. Following the placement of the shield inside the PCB, metallic bonding with the ground is achieved with a solder reflow assembly in a nitrogen oven. Additionally, for some samples, an infrared-heated ball grid array (BGA) rework station machine was employed. Both samples exhibited proper grounding behavior, and both curing systems provided satisfactory results. However, a reflow oven is considered simpler and preferable for larger PCBs due to its scalability and ease of use.

This process can be applied to other shapes, and to the conformal EMI shields as well. The process can be also used to implement compartmentalized and conformal shields

separately or simultaneously. Notably, the T and Inverted L shields are easier to implement compared to the U-shield. That is because they require only one trench compared to the need for two trenches in the U-shape shield. The fabricated and simulated prototypes with a U-shape shield are shown in Fig. 4. Prototypes were designed to operate in the 1-5 GHz range and have a 50  $\Omega$  source and load resistance. The source signal voltage was introduced from a vector network analyzer (VNA, Agilent E5071C), and the testing signal was 1W. The capacitance and inductance between the two microstrips were calculated using (4) and (6). As stated earlier, in this work, we investigated the coupling between the two ICs by representing them as two microstrip lines. However, the concept of prefabricated and assembled EMI shielding can be utilized at both chip and module levels, as shown in Fig. 3.

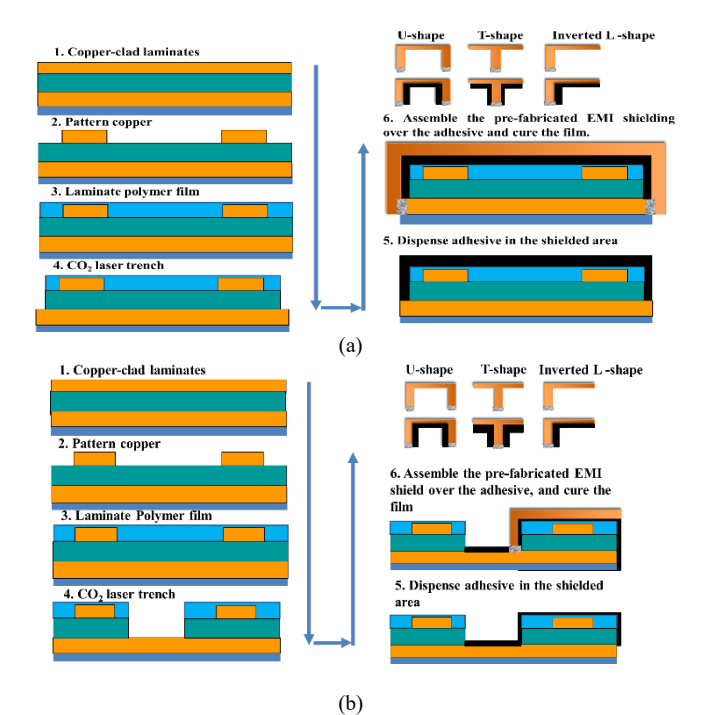


Fig. 3. Process to generate prefabricated and assembled a) conformal, and b) compartment EMI shields.

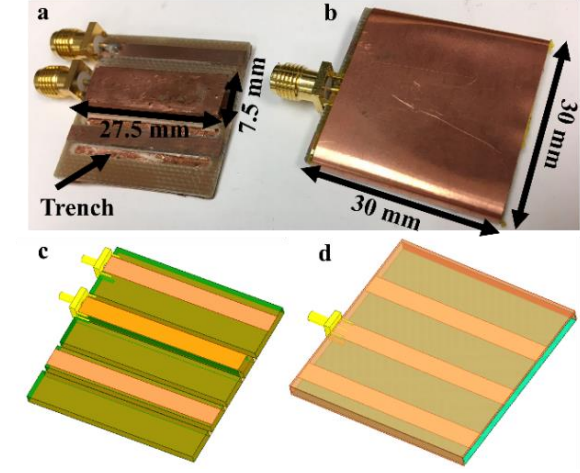


Fig. 4. Fabricated samples on PCB board; a) compartment U-shape, b) conformal U-shape, Simulated samples: c) compartment U-shape, d) conformal U-shape.

The lines and structures were designed specifically to work across 1-5 GHz. Copper as the shield material described in this paper is excellent for blocking EMI at these higher frequencies. For lower frequencies, such as below 1 GHz, it is advantageous to utilize magnetic layers. The challenge with lower frequencies is that the magnetic fields between components get stronger as the impedances are lower. Innovative designs with magnetic materials for EMI shielding become more important. However, the same form factors and designs are adaptable. Since our article mainly talked about copper, the prototypes were made to work best in the higher frequency range.

The surface roughness of the copper in the transmission line measures 2.8 µm. Surface roughness affects the resistance of the transmission lines, with smoother surfaces resulting in lower resistance. While the resistance of each line influences capacitive coupling between components, the shielding's effectiveness remains consistent regardless of TL roughness.

#### IV. CHARACTERIZATION SETUP

Shielding effectiveness (SE) is defined as the difference between the incident and transmitted power through the shield. However, near-field coupling varies between magnetic and electric fields. Hence, it is more specifically defined as the difference between the strengths of the incident and transmitted magnetic or electric fields. Separate set-ups are used for compartmentalized and conformal shields. In this work, and as stated previously, the IC interconnects are represented by two parallel microstrip lines. Shielding is often estimated as S<sub>21</sub> or the insertion loss. The performance of the EMI shield is measured using its SE as the metric. SE is estimated as the difference in the field strength with and without the shield.

## A. Conformal EMI shielding setup.

The SE of conformal EMI shields is determined based on the electric and magnetic field maps. This is illustrated in Fig. 5. Shielding is defined as the ratio of electric (or magnetic field) strengths in the presence and absence of EMI shielding. Field strength is measured using EMC probes, and shielding is thus calculated as:

$$SE_E = 20 \log \frac{|E_{without shield}|}{|E_{with shield}|} \tag{1}$$

$$SE_E = 20 \log \frac{|E_{without shield}|}{|E_{with shield}|}$$
(1)  

$$SE_H = 20 \log \frac{|H_{without shield}|}{|H_{with shield}|}$$
(2)

In the above, E without shield is the received electric field in the absence of the shield, and E with shield is the received electric field in the presence of the shield. Similar definitions follow the magnetic field.

## B. Compartmentalized EMI shielding setup.

Compartmentalized EMI shielding with multiple shapes is implemented on TL2 (see Fig. 1a). A vector network analyzer was used to inject the aggressor signals in TL1 and measure the crosstalk from TL2. This near-end crosstalk is caused by capacitive and magnetic coupling. The measurements were carried out with and without EMI shielding (see Fig. 6). Shielding effectiveness is then determined using.

$$SE = S_{21}(w/o \ shield) - S_{21}(with \ shield)$$
 (3)

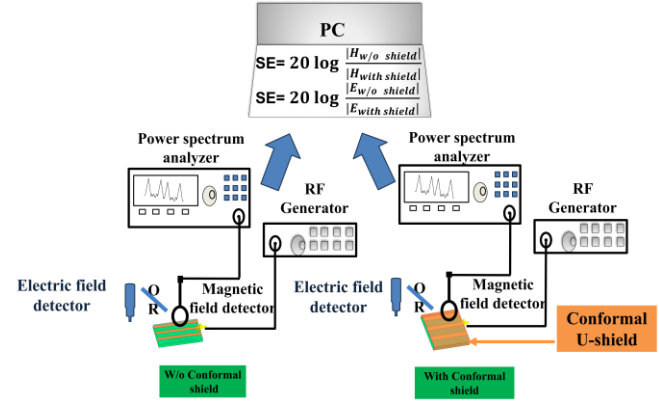


Fig. 5. Measuring EMI shielding effectiveness for magnetic and electric field sources using conformal shields

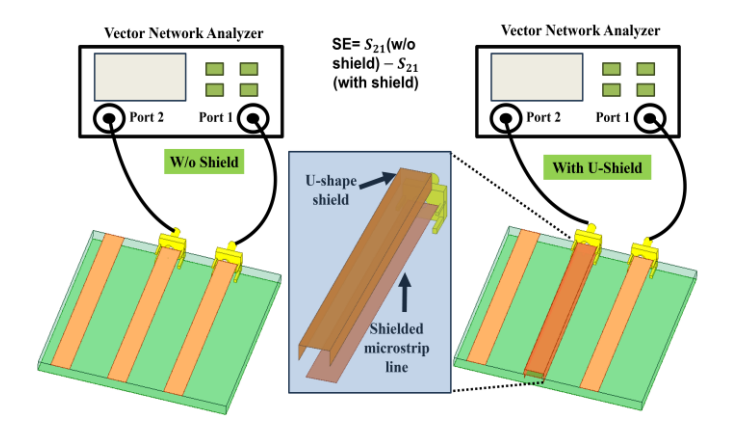


Fig. 6. Measurement and simulation setups for EMI shielding effectiveness with compartmentalized shields.

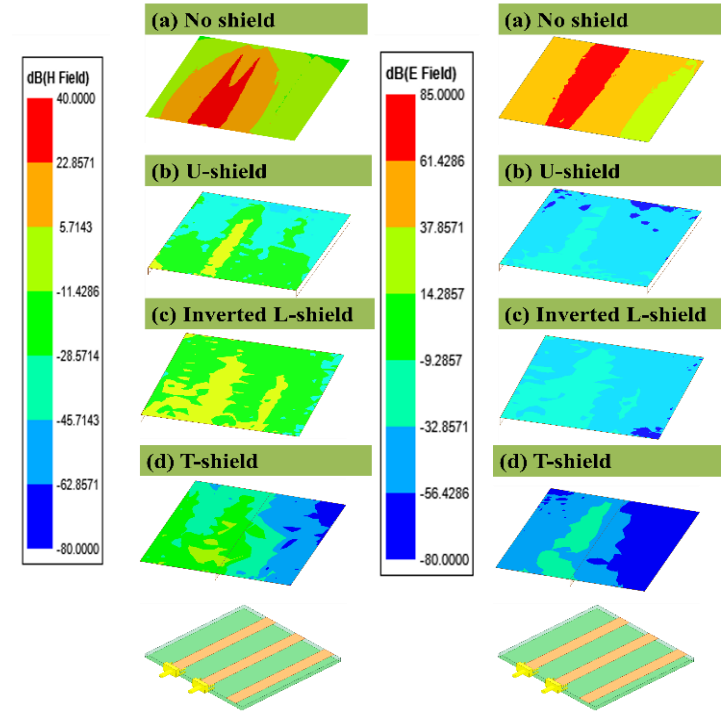


Fig. 7. Magnetic (first column) and electric field (second column) maps at 1 GHz with and without the conformal shield: a) no EMI shield, b) U-shield, c) Inverted L-shape, and d) T-shield. The design variations are illustrated in Fig.

The measurements were conducted in the EMC laboratory at the workbench. Uncontrolled reflective surfaces like metal walls or nearby equipment had minimal impact on the measurements. Since the  $S_{21}$  measurement and near-field probing primarily indicate noise coupling rather than the radiated emissions themselves, conducting them in the EMC workbench laboratory was deemed acceptable. Therefore, there was no necessity to carry out the measurements in a semi- or fully-anechoic chamber.

The purpose of shielding is to suppress noise and emissions from integrated circuits, primarily from digital components. Therefore, shielding typically does not affect transmission line performance, particularly for ICs, which are inherently immune to emissions. However, if shielding were to be placed around analog components such as antennas (although this is unlikely), it could degrade the  $S_{11}$  performance in most cases.

In our study, we focused on the coupling  $(S_{21})$ , which attenuates after implementing the shield between two transmission lines representing scenarios of aggressor and victim components. While the  $S_{11}$  for the shielded line would degrade, we did not address it explicitly since it is representative of cases involving aggressor lines with unwanted harmonics.

#### V. SHIELDING RESULTS AND DISCUSSION

## A. Package-level EMI shielding: U, T, and Inverted L shape shielding.

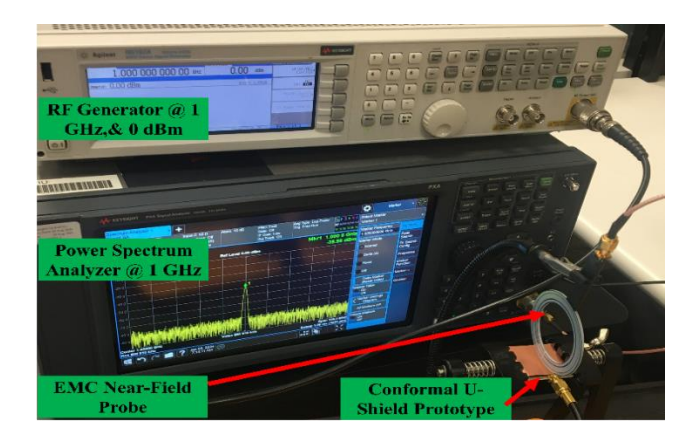
As reviewed in Section I, package-level shielding is predominantly implemented as a conformal shield over multiple components and is usually aimed at isolating noise from internal sources to outside or vice versa. These variations are shown in Fig. 3a. Electric and magnetic field maps are simulated to determine the SE for conformal EMI shielding. These maps were taken at 50 µm distance from the electronic package in the Z (vertical) direction. The electric field strength map for the prototype without conformal shield varied from 30-85 dB (31.622-17,782 V/m) at 1 GHz. In this case, dB scale simply refers to 20 log (field strength). When U-shield was utilized, the field strength varied from -70.5 to -5.5 dB (0.0003 - 0.543 V/m) at 1 GHz. The inverted L-shape resulted in a slightly better performance of -74 to -6 dB (0.0002-0.5 V/m) at the same frequency. We also found that the T-shield showed the best shielding performance of -86 to -6 dB (0.00005-0.5 V/m). However, as shown in the electric field maps in Fig. 7, the performance of the conformal shield near the middle TL is the lowest because of its proximity to the noise source. With increasing distance from TL2, the electric field decreases. Tshape showed the best performance due to its geometry, since the termination wall of the T-shape is closer to TL2 compared to U-shape and Inverted L-shape. This resulted in its improved shielding performance.

As expected, shielding against magnetic fields is more challenging. For example, the simulated magnetic field maps with the conformal shield varied from -21 to 40 dB (0.09 - 100 A/m) at 1 GHz across the plane. The conformal U-shield reduced the magnetic field strength to -54 - 16 dB (0.002 - 6.3 A/m) along the whole plane, especially at 1 GHz. With inverted

L-shields, the fields weakened to -60 - 6 dB (0.001 - 2 A/m). T-shield exhibited the best magnetic field shielding, resulting in a field strength of -82 to 6 dB (0.00008- 2 A/m) at 1 GHz. Its superior performance is due to its geometry, where the wall termination to the ground is closer to the source compared to the other shapes. However, all shapes are effective in suppressing the emission of the electric and magnetic fields in the near-field coupling. The simulated electric and magnetic field maps are illustrated in Fig. 7.

In order to validate the simulation maps of the electric and magnetic fields using the conformal EMI shields, field measurements were performed with EMC probes (Thincol, B08PD7NJ83) (see Fig. 8a). The EMC probes are located at the center of the conformal shield at a distance of 50  $\mu m$ , as illustrated in Fig. 8b. The difference between the magnitude of the fields in the presence and absence of the shield is reported as the SE as given by Equations (1) and (2). All measurements were carried out at 1 GHz. The results, listed in Table II, demonstrate the shield performance in reducing electric and magnetic field emissions.

Measurements were conducted over 4 modules. The standard deviation ranged from 0.5 to 1.2, depending on the shapes. The difference between measurements and simulations was less than 5 dB in the worst cases.



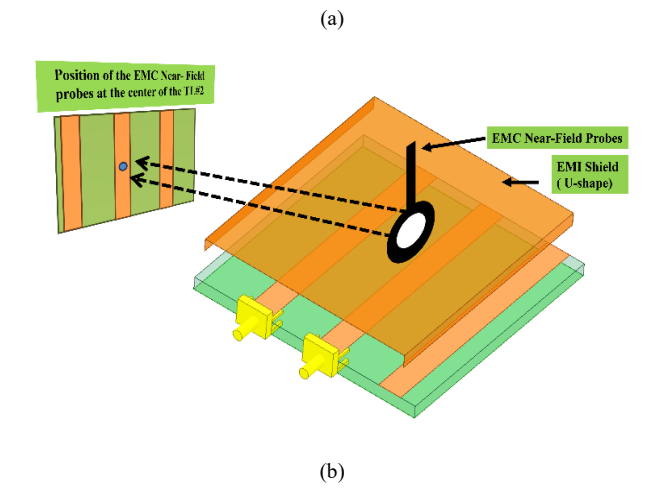


Fig. 8. a) Measurement setup for characterizing conformal EMI shielding against electric and magnetic fields using the EMC probes, b) the position of the EMC near-field probes at the center of the conformal shield.

Table II MEASURED AND SIMULATED SE AT 1 GHz FOR CONFORMAL SHIELDING.

	U-shape	T-shape	Inverted L-shape
	Electric fiel	d SE in dB	
Measurement	64	64	65
Simulation	81	80	80
	Magnetic fie	eld SE in dB	
Measurement	35	43	31
Simulation	43	50	35

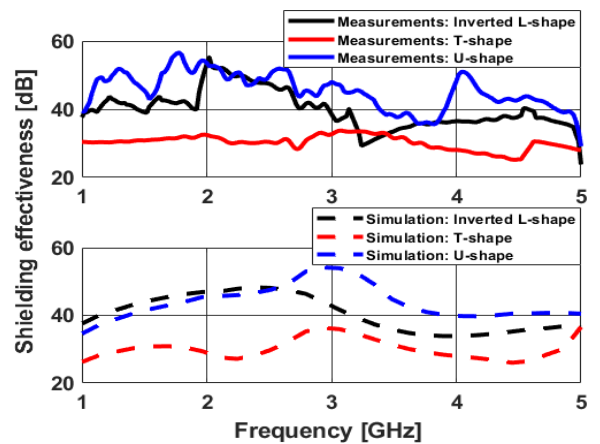


Fig. 9. Simulations and measurements of near-end crosstalk between components with compartmentalized shielding.

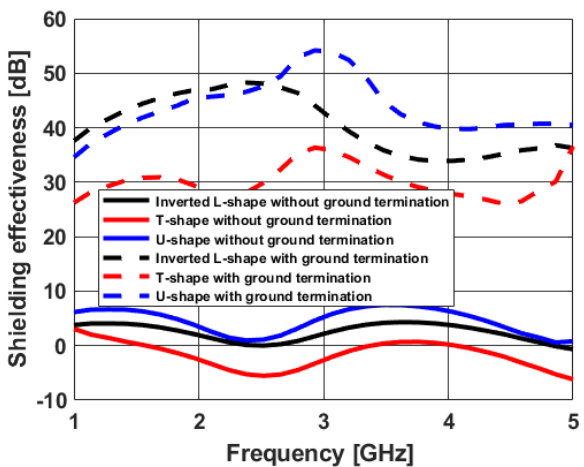


Fig. 10. Simulated isolation results of Inverted L, T, and U- shield of 17.5 $\mu$ m of Cu with and without ground termination.

## B. Component-Level EMI Shielding: U, T, and Inverted L-EMI Shielding Within an Electronic Package.

Prefabricated and assembled shields of 17.5µm Cu designed with U, T, and L variations were used to enhance isolation between TLs, as illustrated in the measurement set-up of Fig. 6. We found that the U-shaped shield reduced the near-end crosstalk by an average of 45 dB across 1-5 GHz. This is verified with both simulations and measurements. The inverted L-shield showed isolation in the range of 35 dB in the same frequency range. In contrast, T- shield showed a lower but impressive shielding of 30 dB between TLs in most of the

frequency range (1-5 GHz). All results from the simulation and measurements are depicted in Fig. 9.

C. Challenges and limitations of prefabricated and assembled EMI shielding solutions with consideration to ground termination.

Our proposed method of prefabricated and assembled EMI shield faces some challenges in achieving optimal performance and compatibility with various electronic systems and packages. The proposed shields typically are fabricated and customized to specific designs. The shields should incorporate specific features such as metal walls and pillars of specific dimensions for a unique package design. The package slots for trenches and vias should be tolerant of misalignment with the shield. Post-processing of gap-fill materials is needed to assemble the shields with good mechanical integrity. Another limitation is the scalability of prefabricated shields to accommodate evolving technology trends and miniaturization. As electronic devices continue to shrink in size and increase in complexity, there is a growing demand for EMI shielding solutions that can effectively address these scaling of design rules. Fortunately, IC assembly rules are shrinking to 5-50 µm with tolerances of 1-5 µm. Prefabricated shields may benefit from these technology trends to meet the tolerance and design rules for heterogeneous package integration where components may be spaced within 100 μm. Finally, our proposed method of EMI shielding comes after the production phase or testing phase, which adds a lot of flexibility to the designers. However, that comes with the challenge of maintaining a good termination to the ground plane. It also needs assembly by heating the solder or silver paste that is used to ensure a good metallic connection between the shield and the ground planes. In summary, prefabricated EMI shields offer valuable benefits in EMI mitigation. The fabrication and assembly scaling will address the challenges related to compatibility, assembly with scalable pitches and tolerances, and ground termination.

Achieving optimal termination hinges on establishing a strong connection between the shield and the ground plane. The contact resistance plays a crucial role in ensuring a solid termination to the ground, as depicted in Fig. 10. The termination or grounding of the shield is important as mentioned in Section II. Fig. 10 compares the simulated shielding performance of Inverted L, T, and U-shapes constructed from 17.5 µm thick Cu with and without ground terminations. Various techniques, including soldering, silver paste application, or other methods such as wire bonding can be employed to effectively achieve this connection. We found that when the prefabricated EMI shields are connected to the ground plane, the EMI shielding showed a reasonable isolation of 40-50 dB. However, the ungrounded EMI shields provided an isolation of only 5-10 dB across the same frequency range. The isolation dropped by 30-40 dB across 1-5 GHz, and the impact of the shield is very weak when isolated from the ground plane.

While maintaining low impedance connections becomes more challenging at higher frequencies, for shielding against most noise emissions, any of the aforementioned methods would provide the desired performance.

The results, thus, demonstrate the effectiveness of the

innovative shielding approach with prefabrication and assembly. Although the current work utilizes semi-manual techniques such as dicing and bonding to pre-fabricate the shields, standard microfabrication approaches such as highaspect ratio copper plating and dicing can further scale down the dimensions and increase the tolerance. Package assembly techniques can reach pitches far below the dimensions needed for the current shield assembly needs. The unique approach developed in this work can thus benefit and become more effective with future microassembly advances. The shields are further thinned down with advances in materials with higher shielding effectiveness. These materials are critical in shielding magnetic fields as they present more challenges compared to electric fields. For example, Table II shows that electric field isolation for conformal shield is 20-40 dB higher compared to that of magnetic fields. Shielding magnetic fields at low frequencies needs innovative material stacks to enhance the shield effectiveness. Monolithic copper can be replaced with multilayered, yet, conducting shields of magnetic nonmagnetic materials that have strong impedance mismatch from magnetic permeabilities. Such materials can scale down the shield geometries to below 10 µm [29]. By utilizing such materials in the microfabrication techniques in conjunction with the preassembly and microassembly techniques described in this work, compartmentalized and package-level shielding can be achieved with scalable system geometries.

This paper primarily focuses on prefabricated EMI shielding, which is best suited for larger dimensions, particularly at the die or IC package level. However, for thinner transmission lines, which are typically rare to shield, alternative techniques can be considered. In scenarios where shielding is necessary but space constraints are present, designing the shield as an integral part of the system rather than adding it onto the design afterward could be a viable approach. This integrated design approach allows for more efficient utilization of space while ensuring effective shielding of individual transmission lines.

## VI. CONCLUSIONS

Novel shielding approaches with prefabricated and assembled EMI components were presented and tested to alleviate design and process constraints associated with current approaches. Notably, the shields were preformed and assembled after the completion of the substrate build-up processes. This method helps in the introduction of advanced shielding materials as they do not need to be compatible with substrate and process design rules. It also mitigates the risk of stress and deformations within electronic packages. In addition, by using advanced prefabrication and microassembly techniques, the thickness of the EMI shields can be controlled with microscale precision.

In the case of conformal shields, electric field shielding for the inverted L, T, and U-shapes, provided an average of 80-100 dB at 1 GHz under near-field coupling. Notably, conformal shields were less effective against magnetic fields. The Conformal U shape shield exhibited an average of 24-53 dB of shielding against magnetic field at 1 GHz as compared to the Inverted L-shape with 34-35 and the T-shape with 34-60 dB.

Monolithic Cu,17.5  $\mu$ m thick, was used in inverted L, T, and U-shape compartmentalized shields to suppress magnetic and electric field coupling (crosstalk coupling) between ICs. Shield performances were compared with a pair of parallel microstrip lines as the test structures. The T-shield reduced crosstalk between TLs by 30 dB across 1-5 GHz, while the inverted L-shape led to an average shielding of 40 dB. Overall, for crosstalk coupling mitigation, the U-shield gave the best performance of 40-50 dB across 1-5 GHz. Also, it was remarked that the grounding of the EMI shields is critical to achieve high performance.

#### ACKNOWLEDGMENT

This work was partly supported by Applied Materials Inc. Parts of this work were also supported bythe NSF grant 2052764.

#### REFERENCES

- [1] H. W. Ott, Electromagnetic compatibility engineering. John Wiley & Sons, 2011.
- [2] C. R. Paul, R. C. Scully, and M. A. Steffka, Introduction to electromagnetic compatibility. John Wiley & Sons, 2022.
- [3] X.-C. Wei, Modeling and design of electromagnetic compatibility for high-speed printed circuit boards and packaging. CRC Press, 2017.
- [4] Y.-S. Choi, Y.-H. Yoo, J.-G. Kim, and S.-H. Kim, "A comparison of the corrosion resistance of Cu–Ni–stainless steel multilayers used for EMI shielding," *Surface and Coatings Technology*, vol. 201, no. 6, pp. 3775-3782, 2006.
- [5] F.-C. Chu, H.-C. Kuo, and C.-C. Wang, "Lowering coupling noise between chips in System-in-Package (SiP) module using compartment shielding," in 2016 11th International Microsystems, Packaging, Assembly and Circuits Technology Conference (IMPACT), 2016: IEEE, pp. 152-155.
- [6] C.-H. Huang, C.-Y. Hsiao, C.-D. Wang, T. Chen, L. Kuo-Hsien, and T.-L. Wu, "Conformal shielding investigation for SiP modules," in 2010 IEEE Electrical Design of Advanced Package & Systems Symposium, 2010: IEEE, pp. 1-4.
- [7] M.-W. Liao, A. Lin, and C.-Y. Huang, "A new resonanceeliminating EMI conformal shielding with side-wall openings," in 2017 12th International Microsystems, Packaging, Assembly and Circuits Technology Conference (IMPACT), 2017: IEEE, pp. 118-121.
- [8] X. Zhang, B. Zhang, and R. Sun, "Effective Conformal EMI Shielding Coating for SiP modules with Multi-shaped Nano-Ag Fillers," in 2022 23rd International Conference on Electronic Packaging Technology (ICEPT), 2022: IEEE, pp. 1-4.
- [9] X. Hong *et al.*, "Compartmental EMI Shielding with Jet-Dispensed Material Technology," in *2019 IEEE 69th Electronic Components and Technology Conference (ECTC)*, 2019: IEEE, pp. 753-757.
- [10] H. Chang, J. Chen, V. Chen, S. Leou, and T. Wang, "Novel multiple compartments shielding for high performance RF design—LTE modem SiP," in 2014 9th International Microsystems, Packaging, Assembly and Circuits Technology Conference (IMPACT), 2014: IEEE, pp. 200-203.
- [11] J.-D. V. Hoang, R. Darveaux, T. LoBianco, Y. Liu, and W. Nguyen, "Breakthrough packaging level shielding techniques and EMI effectiveness modeling and characterization," in 2016 IEEE 66th Electronic Components and Technology Conference (ECTC), 2016: IEEE, pp. 1290-1296.
- [12] S. Sitaraman, J. Min, M. R. Pulugurtha, M. S. Kim, V. Sundaram, and R. Tummala, "Modeling, design and demonstration of

- integrated electromagnetic shielding for miniaturized RF SOP glass packages," in 2015 IEEE 65th Electronic Components and Technology Conference (ECTC), 2015: IEEE, pp. 1956-1960.
- [13] C.-Y. Hsiao *et al.*, "Mold-based compartment shielding to mitigate the intra-system coupled noise on SiP modules," in *2011 IEEE International Symposium on Electromagnetic Compatibility*, 2011: IEEE, pp. 341-344.
- [14] S. Radu and D. Hockanson, "An investigation of PCB radiated emissions from simultaneous switching noise," in 1999 IEEE International Symposium on Electromagnetic Compatability. Symposium Record (Cat. No. 99CH36261), 1999, vol. 2: IEEE, pp. 893-898
- [15] D. M. Hockanson, X. Ye, J. L. Drewniak, T. H. Hubing, T. P. Van Doren, and R. E. DuBroff, "FDTD and experimental investigation of EMI from stacked-card PCB configurations," *IEEE transactions* on electromagnetic compatibility, vol. 43, no. 1, pp. 1-10, 2001.
- [16] K. Mukai, B. Eastep, K. Kim, L. Gaherty, and A. Kashyap, "A new reliable adhesion enhancement process for directly plating on molding compounds for package level EMI shielding," in 2016 IEEE 66th Electronic Components and Technology Conference (ECTC), 2016: IEEE, pp. 1530-1537.
- [17] N. Karim, J. Mao, and J. Fan, "Improving electromagnetic compatibility performance of packages and SiP modules using a conformal shielding solution," in 2010 Asia-Pacific International Symposium on Electromagnetic Compatibility, 2010: IEEE, pp. 56-59.
- [18] F. Jiang, M. Li, and L. Gao, "Research on conformal EMI shielding Cu/Ni layers on package," in 2014 15th International Conference on Electronic Packaging Technology, 2014: IEEE, pp. 227-230.
- [19] H. C. Kuo, C. W. Kuo, and C. C. Wang, "Effective low-frequency EMI conformal shielding for system-in-package (SiP) modules," *Microwave and Optical Technology Letters*, vol. 65, no. 7, pp. 1892-1897, 2023.
- [20] H. Rahman, P. Saha, J. Dowling, and T. Curran, "Shielding effectiveness measurement techniques for various materials used for EMI shielding," in *IEE Colloquium on Screening of Connectors*, Cables and Enclosures, 1992: IET, pp. 9/1-9/6.
- [21] X. Cao, A. Sun, D. Maslyk, J. Gao, Q. Zhuo, and J. Choi, "Effective EMI shielding for semiconductor packages through novel conformal coating," in 2018 China Semiconductor Technology International Conference (CSTIC), 2018: IEEE, pp. 1-5.
- [22] K. Joo *et al.*, "Evaluation of package-level EMI shielding using conformally coated conductive and magnetic materials in low and high frequency ranges," in *2020 IEEE 70th Electronic Components and Technology Conference (ECTC)*, 2020: IEEE, pp. 647-652.
- [23] A. Lin, V. Chen, J. Chen, S. Leou, T. Wang, and H. Chang, "Electrical performance characterization for novel multiple compartments shielding and verification on LTE modem SiP," in 2014 IEEE 16th Electronics Packaging Technology Conference (EPTC), 2014: IEEE, pp. 246-249.
- [24] M. Tsai et al., "Alternative Low Cost EMI Shielding Solutions on SiP Module for 5G mmWave Applications," in 2021 IEEE 23rd Electronics Packaging Technology Conference (EPTC), 2021: IEEE, pp. 334-338.
- [25] J. Leou, V. Chen, J. Chen, T. Wang, and H. Chang, "Miniaturized LTE modem SiP using novel multiple compartments shielding," in *IEEE CPMT Symposium Japan 2014*, 2014: IEEE, pp. 51-54.
- [26] M. Özkök, S. Lamprecht, E. Klusmann and H. Hübner, "Adjustable EMI Shielding on Electronic Packages Realized by Electrolytic Plating," 2019 IEEE CPMT Symposium Japan (ICSJ), Kyoto, Japan, 2019, pp. 191-194, doi: 10.1109/ICSJ47124.2019.8998721.
- [27] Liao Kuo-Hsien, Alex Chi-Hong Chan, Shen Chia Hsien, Lin I-Chia and Huang Hsin Wen, "Novel EMI shielding methodology on highly integration SiP module," 2012 2nd IEEE CPMT Symposium Japan, Kyoto, Japan, 2012, pp. 1-4, doi: 10.1109/ICSJ.2012.6523433.
- [28] L. Liu, J. Gu and B. Wu, "Electromagnetic Interference Shielding Solution For System-In-Package," 2023 China Semiconductor Technology International Conference (CSTIC), Shanghai, China, 2023, pp. 1-4, doi: 10.1109/CSTIC58779.2023.10219218.
- [29] A. O. Watanabe, P. M. Raj, D. Wong, R. Mullapudi, and R. Tummala, "Multilayered electromagnetic interference shielding structures for suppressing magnetic field coupling," *Journal of Electronic Materials*, vol. 47, pp. 5243-5250, 2018.



Ghaleb Saleh Ghaleb Al-Duhni (a student member of IEEE) originating from Irbid, Jordan, was established in 1990. He attained his bachelor's degree in electrical engineering from Yarmouk University in 2012. Subsequently, he pursued a master's degree in Electrical and Electronic Engineering at the University of Texas at the Rio Grande Valley. Currently, he is actively engaged in his Ph.D. in Electrical Engineering at Florida International University, where he leads multiple research thrusts

such as electromagnetic design for EMC, next-generation packaging materials and architectures, and embedded power converters, working with multiple company sponsors. From 2012 to 2017, he held the esteemed position of an electrical engineer in Jordan, and contributed his specialized expertise to a myriad of projects spanning power electronics, and electronic systems. Presently, his primary research endeavors center around the dynamic fields of EMC, passive components, and power electronics, epitomizing his dedication to advancing the frontier of electronics. His research led to 3 patents and >12 publications.



Mudit Khasgiwala has been the Director of RF/Analog System Architecture within Systems to Materials group in Applied Materials for the past 4 years. His group focusses on 5G/6G, EM, power management and SIPI research and design. He is working on technologies and test characterization vehicles for evaluating advanced packaging and heterogenous integration for the AI HPC data center, Automotive and 6G applications. Prior to Applied Materials, Mudit worked in consumer electronics

industry (likes of Amazon, Apple, Sony Ericsson, and Motorola) mainly designing mobile phones, robots, echo, kindle devices, iPhone, and iPad. In the field of RF system architecture and design, he held many senior and principal roles. Mudit currently owns 11 granted and 11 pending patents and a couple of publications in the field of RF, antenna, battery, EM shielding, IPDs and power management system. He did his bachelor's in electrical engineering from India and MS in EE from NYIT with a major in DSP and RF.



John L. Volakis (S'77-M'82-SM'89-F96) obtained his B.E. Degree, summa cum laude, in 1978 from Youngstown State Univ., Youngstown, Ohio, M.Sc. in 1979 from The Ohio State Univ., Columbus, Ohio and the Ph.D. degree in 1982, also from the Ohio State Univ.

Prof. Volakis started his career at Rockwell International North American Aircraft Operations (1982-84), now Boeing. In 1984, he was appointed

Assistant Professor at The University of Michigan, Ann Arbor, MI, becoming a full Professor in 1994. He also served as the Director of the Radiation Laboratory from 1998 to 2000. From January 2003 to Aug. 2017 he was the Roy and Lois Chope Chair Professor of Engineering at the Ohio State University, Columbus, Ohio and served as the Director of the ElectroScience Laboratory from 2003 to 2016. From 2017-2023 he was the Dean of the College of Engineering and Computing. Since 2023, he is a Professor in the Electrical and Computer Engineering at Florida International University (FIU).

Over the years, he carried out research in computational methods, antennas, wireless communications and propagation, electromagnetic compatibility and interference, design optimization, RF materials, multi-physics engineering, millimeter waves, terahertz and medical sensing. His publications include 9 books, over 450 journal papers and 950 conference papers, 33 book chapters and 32 patents/disclosures. Among his co-authored books are: Approximate Boundary Conditions in Electromagnetics, 1995; Finite Element Methods for Electromagnetics, 1998; 4th and 5th ed. Antenna Engineering Handbook, 2007 and 2019; Small Antennas, 2010; and Integral Equation Methods for Electromagnetics, 2011; Wearable Antennas and Electronics, Artech House, 2022. He has graduated/mentored over 100 doctoral students/post-docs with 44 of them receiving best paper awards at conferences. His service to Professional

Societies include: 2004 President of the IEEE Antennas and Propagation Society (2004), Chair of USNC/URSI Commission B (2015-2017), Chair and Vice Chair of the International Radio Science Union (URSI) Commission B (2017-23), twice the general Chair of the IEEE Antennas and Propagation Symposium, IEEE APS Distinguished Lecturer, IEEE APS Fellows Committee Chair, IEEE-wide Fellows committee member & Associate Editor of several journals. He was listed by ISI among the top 250 most referenced authors (2004). Among his awards are: The Univ. of Michigan College of Engineering Research Excellence award (1993), Scott award from The Ohio State Univ. College of Engineering for Outstanding Academic Achievement (2011), IEEE AP Society C-T. Tai Teaching Excellence award (2011), IEEE Henning Mentoring award (2013), IEEE Antennas & Propagation Distinguished Achievement award (2014), The Ohio State University Distinguished Scholar Award (2016), The Ohio State Univ. ElectroScience Lab. George Sinclair Award (2017), URSI Booker Gold Medal (2020), Advanced Computational Electromagnetics Society Fellow, American Association for the Advancement of Science Fellow, and National Academy of Inventors Fellow (2021)...



Pulugurtha Markondeya Raj earned his B.S. from the Indian Institute of Technology, Kanpur, India, in 1993, M.E. from the Indian Institute of Science, Bangalore, India, 1995, and Ph.D. degree from Rutgers University, Piscataway, NJ, USA, in 1999. He is an Associate Professor with the Department of Biomedical Engineering and Electrical and Computer Engineering at Florida International University, Miami, FL, USA. He co-led several technical thrusts in electronic packaging, working with the whole

electronic ecosystem, which includes semiconductor, packaging, material, tool, and end-user companies. He co-advised and mentored more than 40 graduate students, many of whom are current industry leaders and technology pioneers in the electronic packaging industry, working for Apple Inc., Texas Instruments, Intel Corp., Qualcomm, IBM, Google Inc., Broadcom, and other major electronics companies. He is widely recognized for his contributions in integrated passive components and technology roadmapping, component integration for bioelectronic, power and RF modules, and also for promoting the role of nanomaterials and nanostructures for electronics packaging applications, as evident through his several industry partnerships, invited presentations, publications and awards. His research led to more than 380 publications, which include ~110 journal articles 13 patents awarded with several others pending, 20 book chapters, 16 articles in widely circulated technology magazines, and ~220 conference publications. He received more than 25 best-paper awards. He is an Associate Editor for IEEE Transactions on Components, Packaging, And Manufacturing Technology (T-CPMT) and IEEE Nanotechnology Magazine, and the Co-Chair for the IEEE Nanopackaging Technical Committee, since 2014. He developed industry short courses on electronic module integration technologies with power and RF components, and also on biomedical packaging technologies that integrate latest packaging advances for emerging healthcare needs. He served as the IEEE Distinguished Lecturer from 2020 to 2022, and the General Chair for 3D Power Electronics Integration and Manufacturing, in 2023.